PASJ: Publ. Astron. Soc. Japan , –8 (2008)

The Light-cone Effect on the Clustering Statistics in the Cosmological Redshift Space

Yasushi SUTO,[1,2] Hiromitsu MAGIRA[1]

[1] *Department of Physics, University of Tokyo, Tokyo 113-0033*
E-mail(YS): suto@phys.s.u-tokyo.ac.jp
[2] *Research Center for the Early Universe, School of Science, University of Tokyo, Tokyo 113-0033*
and
Kazuhiro YAMAMOTO
Department of Physics, Hiroshima University, Higashi-Hiroshima 739-8526

(Received 1999 October 26; accepted 1999 December 14)

Abstract

We present a theoretical formalism to predict the two-point clustering statistics (the power spectrum and the two-point correlation function), *simultaneously* taking account of the linear velocity distortion, the nonlinear velocity distortion (finger-of-god), the cosmological redshift-space distortion and the light-cone effect. To demonstrate the importance of these effects in exploring the clustering of objects at high redshifts, we show several model predictions for magnitude-limited surveys of galaxies and quasars. This methodology provides a quantitative tool to confront theoretical models against the upcoming precision data on clustering in the universe.

Key words: Cosmology: dark matter — Distance scale — Large-scale structure of universe — Theory — Galaxies: distances and redshifts

1. Introduction

Observations of clustering of the high-redshift universe suffer from a variety of *contaminations* including the linear redshift-space (velocity) distortion (Kaiser 1987; Hamilton 1998), the nonlinear redshift-space (velocity) distortion (Davis & Peebles 1983; Suto & Suginohara 1991; Cole, Fisher, & Weinberg 1994, 1995), the cosmological redshift-space (geometrical) distortion (Alcock & Paczyński 1979; Ballinger, Peacock, & Heavens 1996; Matsubara & Suto 1996), and the cosmological light-cone effect (Matsubara, Suto, & Szapudi 1997; Matarese et al. 1997; Nakamura, Matsubara, & Suto 1998; Moscardini et al. 1998; de Laix & Starkman 1998; Yamamoto & Suto 1999; Suto et al. 1999; Nishioka & Yamamoto 1999).

These effects have been already discussed in the previous papers quoted above, although separately and not in a unified fashion. In particular, Yamamoto, Nishioka, & Suto (1999) derived a formula for the power spectrum which takes account of the three effects except the cosmological redshift-space distortion, while Magira, Jing, & Suto (2000) extensively discussed the first three effects albeit neglecting the cosmological light-cone effect. The former approach requires to specify the (correct) values of both the density parameter Ω_0 and the cosmological constant λ_0 (see also Nishioka & Yamamoto 2000), and the latter analysis is applicable only for data over a narrow range of redshift (i.e., $\Delta z/z \ll 1$).

In this Paper, we develop for the first time the relevant formulae for two-point clustering statistics (the power spectrum and its Fourier transform, the two-point correlation function) which properly incorporate all the four effects mentioned above. To demonstrate the importance of these effects in exploring the clustering of objects at high redshifts, we present the predictions for future redshift surveys of galaxies and quasars, assuming spatially-flat cold dark matter (CDM) cosmology as a representative model.

2. Formulae for the Two-point Clustering Statistics on a Light-cone in the Cosmological Redshift Space

Our method to predict the two-point clustering statistics of objects on a light-cone in the cosmological redshift space proceeds as follows. First we have to specify the model of bias which relates the density field of objects,

$\delta(\mathbf{x}, z)$, to that of mass $\delta_{\rm mass}(\mathbf{x}, z)$. Our formulation presented here assumes the linear bias model (§2.1). While the realistic bias model is not well understood yet, the linear bias model is a fairly good approximation on large scales independently of the details of the biasing mechanism (e.g., Coles 1993, Matsubara 1999). Second, we take into account the redshift-space distortion induced by the peculiar velocity field (§2.2), using both linear theory (Kaiser 1987) and a non-linear modeling for the finger-of-god effect (Peacock & Dodd 1996). Third, we correct for the anisotropy due to the geometry of the universe (§2.3). The resulting anisotropic power spectra are expanded in multipoles and translated to the corresponding moments of the two-point correlation functions (§2.4). Finally those multipoles defined at a given redshift are integrated over the past light-cone with the appropriate weight (§2.5), which yield the final expressions for the two-point clustering statistics of objects on a light-cone in the cosmological redshift space.

2.1. model of bias

Since we are mainly interested in the relation between the two-point statistics on a constant-time hypersurface in the real space and that on a light-cone hypersurface in the cosmological redshift space, we do not adopt a realistic, and consequently too complicated, model of bias. Rather we consider the case of the deterministic, linear and scale-independent bias:

$$\delta(\mathbf{x}, z) = b(z)\ \delta_{\rm mass}(\mathbf{x}, z), \tag{1}$$

although the real bias might be scale-dependent, nonlinear and stochastic to some extent (e.g., Taruya, Koyama, & Soda 1999; Dekel & Lahav 1999; Matsubara 1999). Throughout the Paper, we explicitly use the subscript, mass, to indicate the quantities related to the mass density field, and those without the subscript correspond to the objects satisfying equation (1).

2.2. redshift-space distortion due to the peculiar velocity

The power spectrum distorted by the peculiar velocity field (neglecting the cosmological distortion for the moment), $P^{(S)}(k; z)$, is known to be well approximated by the following expression (Cole et al. 1995; Peacock & Dodds 1996):

$$P^{(S)}(k_\perp, k_\parallel; z) = b^2(z) P^{(R)}_{\rm mass}(k; z) \times \left[1 + \beta(z)\left(\frac{k_\parallel}{k}\right)^2\right]^2 D\left[k_\parallel \sigma_{\rm P}(z)\right], \tag{2}$$

where $k_\perp$ and $k_\parallel$ are the comoving wavenumber perpendicular and parallel to the line-of-sight of an observer, and $P^{(R)}_{\rm mass}(k; z)$ is the mass power spectrum in real space. The second factor in the right-hand-side of equation (2) represents the linear redshift-space distortion derived by Kaiser (1987) adopting the distant-observer approximation and the scale-independent deterministic linear bias. The parameter $\beta(z)$ is defined by

$$\beta(z) \equiv \frac{1}{b(z)}\frac{d\ln D_+(z)}{d\ln a} \simeq \frac{1}{b(z)}\left[\Omega^{0.6}(z) + \frac{\lambda(z)}{70}\left(1 + \frac{\Omega(z)}{2}\right)\right], \tag{3}$$

where $D_+(z)$ is the gravitational growth rate of the linear density fluctuations, and a is the cosmic scale factor. In the above, we introduce the density parameter, the cosmological constant, and the Hubble parameter at redshift z, which are related to their present values respectively as

$$\Omega(z) = \left[\frac{H_0}{H(z)}\right]^2 (1+z)^3 \Omega_0, \quad \lambda(z) = \left[\frac{H_0}{H(z)}\right]^2 \lambda_0, \tag{4}$$

$$H(z) = H_0 \sqrt{\Omega_0 (1+z)^3 + (1 - \Omega_0 - \lambda_0)(1+z)^2 + \lambda_0}. \tag{5}$$

For definiteness we adopt an exponential distribution function for the pairwise peculiar velocity:

$$f_v(v_{12}) = \frac{1}{\sqrt{2}\sigma_{\rm P}} \exp\left(-\frac{\sqrt{2}|v_{12}|}{\sigma_{\rm P}}\right), \tag{6}$$

which leads to the damping function in k-space:

$$D[k\mu\sigma_{\rm P}] = \frac{1}{1 + (k\mu\sigma_{\rm P})^2/2}, \tag{7}$$

with $\sigma_{\rm P}$ being the 1-dimensional pair-wise peculiar velocity dispersion.

2.3. redshift-space distortion due to the geometry of the universe

Due to a general relativistic effect through the geometry of the universe, the *observable* separations perpendicular and parallel to the line-of-sight direction, $x_{s\perp} = (c/H_0)z\delta\theta$ and $x_{s\parallel} = (c/H_0)\delta z$, are mapped differently to the corresponding comoving separations in real space $x_\perp$ and $x_\parallel$:

$$x_{s\perp}(z) = x_\perp cz/[H_0(1+z)d_{\rm A}(z)] \equiv x_\perp/c_\perp(z), \qquad x_{s\parallel}(z) = x_\parallel H(z)/H_0 \equiv x_\parallel/c_\parallel(z), \tag{8}$$

with $d_{\rm A}(z)$ being the angular diameter distance (Alcock & Paczyński 1979; Matsubara & Suto 1996). The difference between $c_\perp(z)$ and $c_\parallel(z)$ generates the apparent anisotropy in the clustering statistics which should be isotropic in the comoving space. Specifically, the power spectrum in the cosmological redshift space, $P^{(\rm CRD)}$, is related to $P^{(S)}$ defined in the *comoving* redshift space (eq.[2]) as

$$P^{(\rm CRD)}(k_{s\perp}, k_{s\parallel}; z) = \frac{1}{c_\perp(z)^2 c_\parallel(z)} \times P^{(S)}\left(\frac{k_{s\perp}}{c_\perp(z)}, \frac{k_{s\parallel}}{c_\parallel(z)}; z\right), \tag{9}$$

where the first factor comes from the Jacobian of the volume element $dk_{s\perp}^2 dk_{s\parallel}$, and $k_{s\perp} = c_\perp(z)k_\perp$ and $k_{s\parallel} = c_\parallel(z)k_\parallel$ are the wavenumber (in the cosmological redshift space) perpendicular and parallel to the line-of-sight direction.

Substituting equation (2), equation (9) reduces to

$$\begin{aligned} P^{(\rm CRD)}(k_s, \mu_k; z) &= \frac{b^2(z)}{c_\perp(z)^2 c_\parallel(z)} P^{(R)}_{\rm mass}\left(\frac{k_s}{c_\perp(z)}\sqrt{1+[\frac{1}{\eta(z)^2}-1]\mu_k^2}; z\right) \\ &\times \left[1+\left(\frac{1}{\eta(z)^2}-1\right)\mu_k^2\right]^{-2} \left[1+\left(\frac{1+\beta(z)}{\eta(z)^2}-1\right)\mu_k^2\right]^2 \left[1+\frac{k_s^2\mu_k^2{\sigma_{\rm P}}^2}{2c_\parallel^2(z)}\right]^{-1}, \end{aligned} \tag{10}$$

where we introduce

$$k_s \equiv \sqrt{k_{s\perp}^2 + k_{s\parallel}^2}, \quad \mu_k \equiv k_{s\parallel}/k_s, \quad \eta \equiv c_\parallel/c_\perp, \tag{11}$$

(Ballinger, Peacock, & Heavens 1996; Magira, Jing, & Suto 2000).

The two-point correlation function in the cosmological redshift space, $\xi^{(\rm CRD)}(x_{s\perp}, x_{s\parallel}; z)$, is computed using equation (10) as

$$\begin{aligned} \xi^{(\rm CRD)}(\mathbf{x_s}; z) &= \frac{1}{(2\pi)^3}\int P^{(\rm CRD)}(\mathbf{k_s}; z)\exp(-i\mathbf{k_s}\cdot\mathbf{x_s})d^3k_s \\ &= \frac{1}{(2\pi)^3}\int P^{(S)}(\mathbf{k}; z)\exp(-i\mathbf{k}\cdot\mathbf{x})d^3k \\ &= \xi^{(S)}(c_\perp x_{s\perp}, c_\parallel x_{s\parallel}; z), \end{aligned} \tag{12}$$

where $\xi^{(S)}(x_\perp, x_\parallel; z)$ is the redshift-space correlation function defined through equation (2).

2.4. multipole expansion

Following Hamilton (1992), we decompose the power spectrum into harmonics:

$$P(k, \mu_k; z) = \sum_{l:even} P_l(k)L_l(\mu_k), \quad P_l(k; z) \equiv \frac{2l+1}{2}\int_{-1}^{1} d\mu_k P(k, \mu_k; z)L_l(\mu_k), \tag{13}$$

where μ_k is the direction cosine between the wavevector and the line-of-sight, and $L_l(\mu_k)$ are the l-th order Legendre polynomials. Similarly, the two-point correlation function is decomposed as

$$\xi(x, \mu_x; z) = \sum_{l:even} \xi_l(x)L_l(\mu_x), \quad \xi_l(x; z) \equiv \frac{2l+1}{2}\int_{-1}^{1} d\mu_x \xi(x, \mu_x; z)L_l(\mu_x), \tag{14}$$

using the direction cosine μ_x between the separation vector and the line-of-sight.

The above multipole moments satisfy the following relations:

$$P_l(k; z) = 4\pi i^l \int_0^\infty \xi_l(x; z)j_l(kx)x^2 dx, \quad \xi_l(x; z) = \frac{1}{2\pi^2 i^l}\int_0^\infty P_l(k; z)j_l(kx)k^2 dk, \tag{15}$$

with $j_l(kx)$ being the spherical Bessel functions. Substituting $P^{(\rm CRD)}(k_s, \mu_k; z)$ and $\xi^{(\rm CRD)}(\mathbf{x_s}; z)$ in equations (13) to (15), one can compute the moments, $P_l^{(\rm CRD)}(k_s; z)$ and $\xi_l^{(\rm CRD)}(x_s; z)$ at a given z. Actually the above relations are essential in predicting the two-point correlation function in the cosmological redshift space with the nonlinear effects.

2.5. the light-cone effect

Finally we incorporate the light-cone effect following the expression by Yamamoto & Suto (1999). Since $P_l^{(\rm CRD)}(k_s;z)$ and $\xi_l^{(\rm CRD)}(k_s;z)$ are defined in redshift space, the proper weight should be

$$d^3s^{(\rm CRD)}\ [\phi(z)n_0^{\rm CRD}(z)]^2 = d^3x[\phi(z)n_0^{\rm com}(z)]^2\ c_\perp(z)^2c_\parallel(z), \tag{16}$$

where $n_0^{\rm CRD}(z)$ and $n_0^{\rm com}(z)$ denote number densities of the objects in cosmological redshift space and comoving space, respectively, and $\phi(z)$ is the selection function determined by the observational target selection and the luminosity function of the objects. Then the final expressions reduce to

$$P_l^{(\rm LC,CRD)}(k_s) = \frac{\displaystyle\int_{z_{\rm max}}^{z_{\rm min}} dz\frac{dV_{\rm c}}{dz}\ [\phi(z)n_0^{\rm com}(z)]^2c_\perp(z)^2c_\parallel(z)P_l^{(\rm CRD)}(k_s;z)}{\displaystyle\int_{z_{\rm max}}^{z_{\rm min}} dz\frac{dV_{\rm c}}{dz}\ [\phi(z)n_0^{\rm com}(z)]^2c_\perp(z)^2c_\parallel(z)}, \tag{17}$$

$$\xi_l^{(\rm LC,CRD)}(x_s) = \frac{\displaystyle\int_{z_{\rm max}}^{z_{\rm min}} dz\frac{dV_{\rm c}}{dz}\ [\phi(z)n_0^{\rm com}(z)]^2c_\perp(z)^2c_\parallel(z)\xi_l^{\rm CRD}(x_s;z)}{\displaystyle\int_{z_{\rm max}}^{z_{\rm min}} dz\frac{dV_{\rm c}}{dz}\ [\phi(z)n_0^{\rm com}(z)]^2c_\perp(z)^2c_\parallel(z)}, \tag{18}$$

where $z_{\rm max}$ and $z_{\rm min}$ denote the redshift range of the survey, $dV_{\rm c}/dz = d_{\rm C}^2(z)/H(z)$ is the comoving volume element per unit solid angle.

Note that k_s and x_s defined in $P_l^{(\rm CRD)}(k_s;z)$ and $\xi_l^{\rm CRD}(x_s;z)$ are related to their comoving counterparts at z through equations (11) and (8) while those in $P_l^{(\rm LC,CRD)}(k_s)$ and $\xi_l^{(\rm LC,CRD)}(x_s)$ are not specifically related to any comoving wavenumber and separation. Rather they correspond to the quantities averaged over the range of z satisfying the observable conditions of $x_s = (c/H_0)\sqrt{\delta z^2 + z^2\delta\theta^2}$ and $k_s = 2\pi/x_s$.

3. Predictions for Galaxy and QSO Samples in CDM Models

As in Yamamoto, Nishioka, & Suto (1999), we consider SCDM (standard cold dark matter) and LCDM (Lambda cold dark matter) models, which have $(\Omega_0, \lambda_0, h, \sigma_8) = (1.0, 0.0, 0.5, 0.6)$ and $(0.3, 0.7, 0.7, 1.0)$, respectively. These sets of cosmological parameters are chosen so as to reproduce the observed cluster abundance (Kitayama & Suto 1997). We use the fitting formulae of Peacock & Dodds (1996) and Mo, Jing, & Börner (1997) for the nonlinear power spectrum $P_{\rm mass}^{(R)}(k;z)$ and the peculiar velocity dispersions $\sigma_{\rm P}$, respectively (see also Suto et al. 1999; Magira et al. 2000). Also we take into account the selection functions relevant to the upcoming SDSS spectroscopic samples of galaxies and quasars adopting the B-band limiting magnitudes of 19 and 20, respectively. Unlike Yamamoto & Suto (1999) and Yamamoto, Nishioka, & Suto (1999), we properly transform the QSO luminosity function originally fitted assuming the Einstein – de Sitter universe (Wallington & Narayan 1993; Nakamura & Suto 1997) to that in a given cosmological model.

Figure 1 compares the predictions for the angle-averaged (monopole) power spectra under various approximations. Upper and lower panels adopt the selection functions appropriate for galaxies in $0 < z < z_{\rm max} = 0.2$ and QSOs in $0 < z < z_{\rm max} = 5$, respectively. Left and right panels present the results in SCDM and LCDM models. For simplicity we adopt a scale-independent linear bias model of Fry (1996):

$$b(z) = 1 + \frac{1}{D_+(z)}[b(k, z=0) - 1], \tag{19}$$

with $b(k, z = 0) = 1$ and 1.5 for galaxies and quasars, respectively. We present the results normalized by the real-space power spectrum in linear theory (Bardeen et al. 1986); $P_0^{(\rm S)}(k;z=0)$, $P_0^{(\rm S)}(k;z=z_{\rm max})$, $P_0^{(\rm CRD)}(k_s;z=z_{\rm max})$, and $P_0^{(\rm LC,CRD)}(k_s)$ are computed using the nonlinear power spectrum of Peacock & Dodds (1996), and plotted in dashed, dash-dotted, dotted and solid lines, respectively.

Consider the results for the galaxy sample (upper panels) first. On linear scales ($k < 0.1h{\rm Mpc}^{-1}$), $P_0^{(\rm S)}(k;z=0)$ plotted in dashed lines is enhanced relative to that in real space mainly due to the linear redshift-space distortion (The Kaiser factor in eq.[2]). For nonlinear scales, the nonlinear gravitational evolution increases the power spectrum in real space while the finger-of-god effect suppresses that in redshift space. Thus the net result is sensitive to the shape and the amplitude of the fluctuation spectrum itself; in the LCDM model that we adopted, the nonlinear

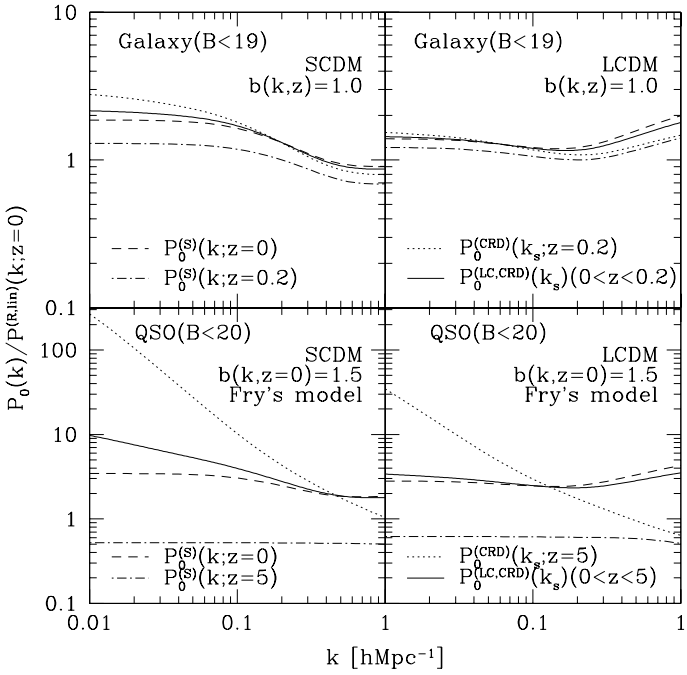

Fig. 1.. The light-cone and cosmological redshift-space distortion effects on angle-averaged power spectra. Upper and lower panels correspond to magnitude-limited samples of galaxies ($B < 19$ in $0 < z < z_{\rm max} = 0.2$; no bias model) and QSOs ($B < 20$ in $0 < z < z_{\rm max} = 5$; Fry's linear bias model), respectively. *Dashed*: $P_0^{(\rm S)}(k; z = 0)/P^{(\rm R,lin)}(k; z = 0)$, *dash-dotted*: $P_0^{(\rm S)}(k; z = z_{\rm max})$, *dotted*: $P_0^{(\rm CRD)}(k_s; z = z_{\rm max})$, *solid*: $P_0^{(\rm LC,CRD)}(k_s)$.

gravitational growth in real space is stronger than the suppression due to the finger-of-god effect. Thus $P_0^{(\rm S)}(k; z = 0)$ becomes larger than its real-space counterpart in linear theory. In the SCDM mode, however, this is opposite and $P_0^{(\rm S)}(k; z = 0)$ becomes smaller.

The power spectra at $z = 0.2$ (dash-dotted lines) are smaller than those at $z = 0$ by the corresponding growth factor of the fluctuations, and one might expect that the amplitude of the power spectra on the light-cone (solid lines) would be in-between the two. While this is correct if we use the comoving wavenumber, the actual observation on the light-cone in the cosmological redshift space should be expressed in terms of k_s (eq.[(11]). If we plot the power spectra at $z = 0.2$ taking into account the geometrical distortion, $P_0^{(\rm CRD)}(k_s; z = 0.2)$ in dotted lines becomes significantly larger than $P_0^{(\rm S)}(k; z = 0.2)$. Therefore $P_0^{(\rm LC,CRD)}(k_s)$ should take a value between those of $P_0^{(\rm CRD)}(k_s; z = 0) = P_0^{(\rm S)}(k; z = 0)$ and $P_0^{(\rm CRD)}(k_s; z = 0.2)$. This explains the qualitatively features shown in upper panels of figure 1. As a result, both the cosmological redshift-space distortion and the light-cone effect substantially change the predicted shape and amplitude of the power spectra, even for the galaxy sample (Nakamura, Matsubara, & Suto 1998).

The results for the QSO sample can be basically understood in a similar manner except that the evolution of bias makes significant difference since the sample extends to much higher redshifts. Although it is true that the results are sensitive to the model of bias, we believe that those on linear scales are fairly insensitive to the complexities of the bias; it has been shown that the bias on such scales can be well approximated by the linear and scale-independent model (Coles 1993; Matsubara 1999; Magira, Taruya, Jing & Suto 2000).

Figure 2 shows the results for the angle-averaged (monopole) two-point correlation functions, exactly corresponding to those in figure 1. The results in this figure can be also understood by the analogy of those presented in figure 1 at $k \sim 2\pi/x$. Unlike the power spectra, however, two-point correlation functions are not positive definite. The funny features in figure 2 on scales larger than $30h^{-1}$Mpc ($100h^{-1}$Mpc) in SCDM (LCDM) originate from the fact that $\xi^{(\rm R,lin)}(x, z = 0)$ becomes negative there.

In the linear and deterministic bias model that we adopted here, the power spectra of objects at z in redshift space (without the geometrical effect) are proportional to the mass power spectrum in real space, $P_{\rm mass}^{(R)}(k; z)$. Hamilton

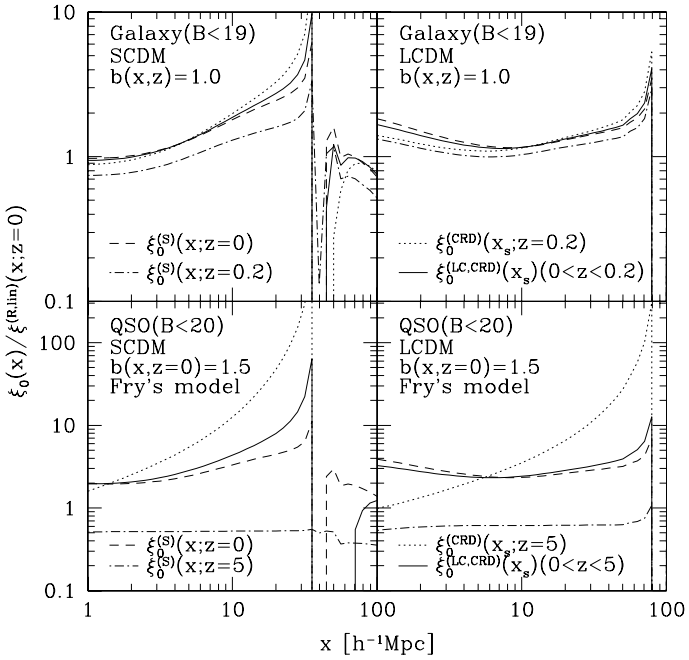

Fig. 2.. The same as Fig.1. on angle-averaged two-point correlation functions.

(1992) showed that in linear theory of redshift-space distortion (Kaiser 1987), the quadrupole to monopole ratio provides a measure of estimating β through the following relation:

$$\frac{P_2^{\rm S,lin}(k;z)}{P_0^{\rm S,lin}(k;z)} = \frac{\frac{4}{3}\beta(z)+\frac{4}{7}\beta^2(z)}{1+\frac{2}{3}\beta(z)+\frac{1}{5}\beta^2(z)} = \frac{\xi_2^{\rm S,lin}(x;z)}{\xi_0^{\rm S,lin}(x;z)-3\int_0^1 \xi_0^{\rm S,lin}(xw;z)w^2dw}. \tag{20}$$

Taking account of the nonlinear redshift-space distortion, however, the ratio becomes scale-dependent; our present model (2) with equation (7) yields

$$\frac{P_2^{\rm S}(k;z)}{P_0^{\rm S}(k;z)} = \frac{\frac{5}{2}\left[B(\kappa)-A(\kappa)\right]+\beta(z)\left[3C(\kappa)-\frac{5}{3}B(\kappa)\right]+\beta^2(z)\left[\frac{3}{2\kappa^2}(1-C(\kappa))-\frac{1}{2}C(\kappa)\right]}{A(\kappa)+\frac{2}{3}\beta(z)B(\kappa)+\frac{1}{5}\beta^2(z)C(\kappa)}, \tag{21}$$

$$A(\kappa) = \frac{\arctan(\kappa)}{\kappa}, \quad B(\kappa)=\frac{3}{\kappa^2}\left[1-\frac{\arctan(\kappa)}{\kappa}\right], \quad C(\kappa)=\frac{5}{3\kappa^2}\left[1-\frac{3}{\kappa^2}+\frac{3\arctan(\kappa)}{\kappa^3}\right], \tag{22}$$

with $\kappa(z)=k\sigma_{\rm P}(z)/\sqrt{2}H_0$ (Magira, Jing, & Suto 2000; Yamamoto, Nishioka, & Suto 1999; see also Cole, Fisher, & Weinberg 1995). We note here that $P_2^{\rm S}(k;z)$ is not any more positive definite and in fact changes sign at cosmologically interesting scales (see figure 3 below).

The above ratio of monopole and quadrupole turns out to be independent of the underlying mass power spectrum, which is regarded as one of the advantages of estimating the β-parameter using the redshift-space distortion. The cosmological redshift-space distortion (eqs.[10] and [13]) and the light-cone effect (eqs.[17] and [18]), however, further complicate the behavior of the final predictions for the two-point statistics, which are plotted in figure 3. In fact, even the shape of $P_0^{\rm (LC,CRD)}(k_s)$ and $P_2^{\rm (LC,CRD)}(k_s)$ for QSOs is sensitive to the bias model and the cosmological parameters.

For the galaxy sample, $P_2^{\rm (LC,CRD)}(k_s)/P_0^{\rm (LC,CRD)}(k_s)$ in large scales approaches 1.06 (0.65) for SCDM (LCDM), which should be compared with 50/49 (0.57) in linear theory (eq.[20]). This implies that such estimated values of β are 1.05 (0.57), in contrast to the true values of 1.0 (0.49). Thus even for the shallow samples of galaxies, the present effects systematically changes the estimate of β by $(5\sim 20)\%$ level (Nakamura, Matsubara, & Suto 1998).

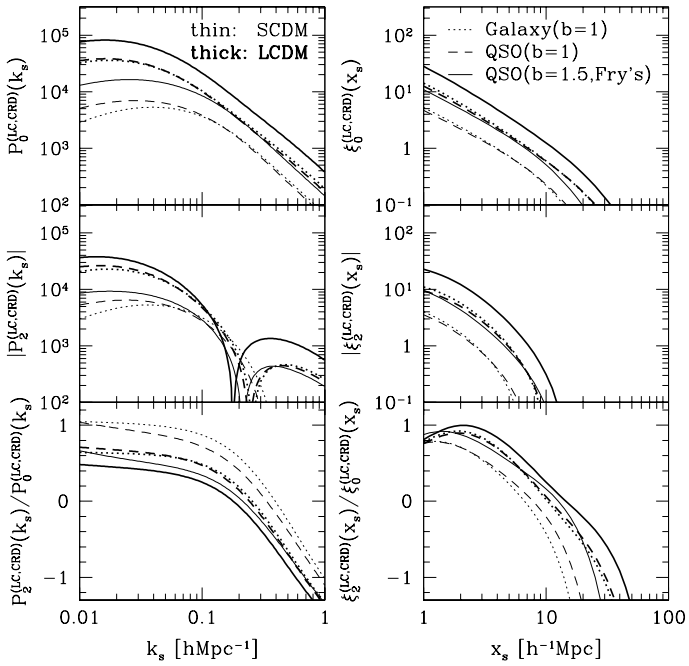

Fig. 3.. Predictions for the two-point statistics on a light-cone in the cosmological redshift space. The results in SCDM and LCDM models are plotted in thin and thick lines, respectively. *Left:* monopole, quadrupole and quadrupole-to-monopole ratio of the power spectrum (from top to bottom). *Right:* monopole, quadrupole and quadrupole-to-monopole ratio of the two-point correlation functions (from top to bottom).

4. Conclusions and Discussion

We have developed for the first time a theoretical formalism to predict the two-point clustering statistics on a light-cone in the cosmological redshift space, $P^{(\mathrm{LC,CRD})}(k_s)$ and $\xi_0^{(\mathrm{LC,CRD})}(x_s)$, which were only discussed separately before (Yamamoto, Nishioka, & Suto 1999; Magira, Jing, & Suto 2000). This methodology fully takes into account all the *well-defined* physical, i.e., gravitational and dynamical effects, and enables one to quantitatively confront the future precision data on the clustering statistics against the cosmological model predictions *modulo* the uncertainty of the bias.

In fact, since the resulting predictions are sensitive to the bias, which is unlikely to quantitatively be specified by theory, the present methodology will find two completely different applications. For relatively shallower catalogues like galaxy samples, the evolution of bias is not supposed to be so strong. Thus one may estimate the cosmological parameters from the observed degree of the redshift distortion as has been conducted conventionally. Most importantly we can correct for the systematics due to the light-cone and geometrical distortion effects which affect the estimate of the parameters by $\sim 10\%$ (§3). This is generally the case on linear and quasi-nonlinear scales where it has been shown that the bias on such scales can be well approximated by the linear and scale-independent model (Coles 1993; Matsubara 1999; Magira, Taruya, Jing & Suto 2000) as we have assumed in this paper.

Alternatively, for deeper catalogues like high-redshift quasar samples, one can extract information on the nonlinearity, scale-dependence and stochasticity of the object-dependent bias (Taruya, Koyama, & Soda 1999; Dekel & Lahav 1999; Blanton et al. 1999) only by correcting the observed data on the basis of our formulae. In this case one should adopt a set of cosmological parameters a priori, but they will be provided both from the low-redshift analysis described above and from the precision data of the cosmic microwave background and supernovae Ia.

In a sense, the former approach uses the light-cone and geometrical distortion effects as real cosmological signals, while the latter regards them as inevitable, but physically removable, noises. In both cases, the present methodology is essential in properly interpreting the observations of the universe at high redshifts.

We thank Shin Sasaki for suggesting the proper scaling of the QSO luminosity function to an arbitrary cosmological model. This research was supported in part by the Grants-in-Aid by the Ministry of Education, Science, Sports and

Culture of Japan to RESCEU (07CE2002) and to K.Y. (11640280), and by the Inamori Foundation.

References

Alcock C., Paczyński B. 1979, Nature 281, 358
Ballinger W.E., Peacock J.A., Heavens A.F. 1996, MNRAS 282, 877
Bardeen J.M., Bond J.R., Kaiser N., Szalay A.S. 1986, ApJ 304, 15
Blanton M., Cen R.Y., Ostriker J.P., Strauss M.A. 1999, ApJ 522, 590
Coles P. 1993, MNRAS 262, 1065
Cole S., Fisher K.B., Weinberg D.H. 1994, MNRAS 267, 785
Cole S., Fisher K.B., Weinberg D.H. 1995, MNRAS 275, 515
Davis M., Peebles P.J.E. 1983, ApJ 267, 465
Dekel A., Lahav O. 1999, ApJ 520, 24
de Laix A.A., Starkman G.D. 1998, MNRAS 299, 977
Fry J.N. 1996, ApJ 461, L65
Hamilton A.J.S. 1992, ApJ 385, L5
Hamilton A.J.S. 1998, The Evolving Universe. Selected Topics on Large-Scale Structure and on the Properties of Galaxies (Kluwer, Dordrecht) p185
Kaiser N. 1987, MNRAS 227, 1
Kitayama T., Suto Y. 1997, ApJ 490, 557
Magira H., Jing Y.P., Suto Y. 2000, ApJ 528, January 1 issue, in press (astro-ph/9907438)
Magira H., Taruya, A., Jing Y.P., Suto Y. 2000, in preparation
Matarrese S., Coles P., Lucchin F., Moscardini L. 1997, MNRAS 286, 115
Matsubara T. 1999, ApJ 525, 543
Matsubara T., Suto Y. 1996, ApJ 470, L1
Matsubara T., Suto Y., Szapudi I. 1997, ApJ 491, L1
Mo H.J., Jing Y.P., Börner G. 1997, MNRAS 286, 979
Moscardini L., Coles P., Lucchin F., Matarrese S. 1998, MNRAS 299, 95
Nakamura T.T., Matsubara T., Suto Y. 1998, ApJ 494, 13
Nakamura T.T., Suto Y. 1997, Prog. Theor. Phys. 97, 49
Nishioka H., Yamamoto K. 1999, ApJ 520, 426
Nishioka H., Yamamoto K. 2000, ApJS, in press
Peacock J.A., Dodds S.J. 1996, MNRAS 280, L19
Suto Y., Magira H., Jing Y.P., Matsubara T., Yamamoto K. 1999, Prog. Theor. Phys. Suppl. 133, 183
Suto Y., Suginohara T. 1991, ApJ 370, L15
Taruya A., Koyama K., Soda J. 1999, ApJ 510, 541
Wallington S., Narayan R. 1993, ApJ 403, 517
Yamamoto K., Nishioka H., Suto Y. 1999, ApJ 527, December 20 issue, in press (astro-ph/9908006)
Yamamoto K., Suto Y. 1999, ApJ 517, 1